Journal of Nanophotonics

SPIEDigitalLibrary.org/jnp

Light scattering with oxide nanocrystallite aggregates for dye-sensitized solar cell application

Qifeng Zhang
Christopher S. Dandeneau
Kwangsuk Park
Dawei Liu
Xiaoyuan Zhou
Yoon-Ha Jeong
Guozhong Cao

Light scattering with oxide nanocrystallite aggregates for dye-sensitized solar cell application

Qifeng Zhang,[a] Christopher S. Dandeneau,[a] Kwangsuk Park,[a] Dawei Liu,[a] Xiaoyuan Zhou,[a] Yoon-Ha Jeong,[b] and Guozhong Cao[a]

[a] University of Washington, Materials Science and Engineering, Seattle, WA 98195, USA
gzcao@u.washington.edu

[b] Pohang University of Science and Technology, National Center for Nanomaterials Technology, Pohang, South Korea

Abstract. Oxide nanocrystallite aggregates are candidates for use in dye-sensitized solar cells. The aggregates are of submicron size, formed by nano-sized crystallites and, therefore, able to offer both a large specific surface area and desirable size comparable to the wavelength of light. While used for a photoelectrode in a dye-sensitized solar cell, the aggregates can be designed to generate effective light scattering and thus extend the traveling distance of light within the photoelectrode film. This would result in an enhancement in the light harvesting efficiency of the photoelectrode and thus an improvement in the power conversion efficiency of the cell. When this notion was applied to dye-sensitized ZnO solar cells, a more than 120% increase in the conversion efficiency was observed with photoelectrode film consisting of ZnO aggregates compared with that comprised of nanocrystallites only. In the case of TiO_2, the photoelectrode film that was formed by TiO_2 aggregates presented conversion efficiency much lower than that obtained for nanocrystalline film. This may be attributed to the non-ideal porosity of the TiO_2 aggregates and the unsuitable facets of the nanocrystallites that form to the aggregates. However, a 21% improvement in the conversion efficiency was still observed for the TiO_2 films including nanocrystallites mixed with 50% aggregates, indicating the effectiveness of the TiO_2 aggregates as light scatterers in dye-sensitized solar cells. Optimization of the structure and the surface chemistry of TiO_2 aggregates, aiming to yield more significant improvement in the conversion efficiency of dye-sensitized solar cells, is necessary.

Keywords: light scattering, dye-sensitized solar cell, aggregates, nanocrystallite.

1. INTRODUCTION

Dye-sensitized solar cells (DSCs) have recently received much attention as a promising alternative to those semiconductor-based solar cells [1-15]. A DSC is essentially a photoelectrochemical system, in which the light harvesting is accomplished by dye molecules that are adsorbed on the surface of the oxide nanostructures that form the photoelectrode film. During operation, photons captured by the dye monolayer create excitons that are rapidly split at the nanocrystallite surface of the oxide film. Electrons are injected into the oxide film and holes are released by the redox couples in the liquid electrolyte. In a DSC, to capture all of the incident photons, the thickness of the photoelectrode film, d, is expected to be larger than the light absorption length, $1/a$, (i.e., $d>1/a$). If such a scenario is realized, the film may have a sufficient surface for dye adsorption and possess optical absorption characteristics near 100%. However, due to the existence of charge recombination in DSCs (which results in a loss of photogenerated electrons during transport) [16, 17], the thickness of the photoelectrode film must be smaller than the electron diffusion length, L_n, (i.e., $d<L_n$). Ideally, all of the photogenerated electrons diffuse through a short distance within the photoelectrode film and reach the transparent anode before recombination occurs. As the photoelectrode film becomes

Received 30 Nov 2009; accepted 30 Apr 2010; published 6 May 2010 [CCC: 19342608/2010/$25.00]

thinner, the energy loss encountered by photogenerated electrons is reduced. Such a dynamic competition between the generation and recombination of electrons has been regarded as a bottleneck that limits the DSCs from achieving conversion efficiencies higher than the 10~11% values that have been obtained for several years [16, 18-20]. Improvement in the light harvesting efficiency (LHE) of the photoelectrode is one approach that may reduce the thickness requirement for the photoelectrode film. Reducing this requirement would serve to lower the recombination rate and boost the performance of DSCs.

One way to improve the LHE of a photoelectrode is a use of new sensitizers with increased absorption coefficients and/or extended long-wavelength absorption edges. Such an approach has led to significant improvements in the conversion efficiency of DSCs. For example, overall conversion efficiencies of 11.0-11.3% have been recently obtained during the preliminary testing of a nanocrystalline TiO_2 film sensitized with C101, a new type of dye [21]. This dye consists of a heteroleptic polypyridyl ruthenium complex, in which the π-conjugation of the spectator ligands is extended and thus, the molecules present a higher molar extinction coefficient (17.5×10^3 $M^{-1}cm^{-1}$) when compared to commercial dyes such as N719 (14.2×10^3 $M^{-1}cm^{-1}$) and Z907 (12.2×10^3 $M^{-1}cm^{-1}$). Other structured ruthenium complexes such as K8 and K9 also show a broad and greatly enhanced spectral response. This response enables a nanocrystalline film with only an 8 μm thickness to reach an overall conversion efficiency as high as 8.2% due to a significant improvement in the LHE [22]. A similar result was also reported using the organic sensitizers JK-1 and JK-2, where an ~8% conversion efficiency on TiO_2 nanocrystalline films was achieved [23].

In addition to the molecular engineering of sensitizers, the effect of light scattering has been also adopted as an effective manner to improve the LHE of the photoelectrode in DSCs. This notion is based on the consideration that light scattering may cause optical reflection or diffusion and can therefore, extend the traveling distance of incident light within a photoelectrode film. Light scattering in DSCs can be realized through the use of either a bilayer structure consisting of a light scattering overlayer and a nanocrystalline TiO_2 film, or by employing a binary combination consisting of a nanocrystalline film mixed with submicron-sized particles. Ferber *et al.* and Usami *et al.* performed theoretical studies on the enhancement effect of light scattering on DSC conversion efficiency [24, 25]. The results indicated that the optical absorption of the photoelectrode could be enhanced by introducing submicron-sized large particles into the nanocrystalline film or by using the large particles as a back-surface scattering layer. However, it was noted that, in addition to optimizing the particle size and the ratio of nanoparticles to large particles, the film thickness for each layer must also be optimized so as to compensate for a simultaneous decrease in the internal surface area of photoelectrode film. In practice, a lot of studies have reported to improve the DSC performance using nanocrystalline TiO_2 film in corporation with submicron-sized large particles as light scatterers [18, 26-28]. Furthermore, a layer of scattering film consisting of TiO_2 with dimensions of 300-400 nm has also been widely employed in a traditional DSC to reflect the incident light [29-38]. Such a film is fabricated on the back of the nanocrystalline film. In other studies aimed at generating light scattering and enhancing the LHE of a photoelectrode film, researchers have reported on the use of a photonic crystal layer or spherical voids that were embedded in a nanocrystalline film [39-47]. However, these methods have the disadvantage of causing an unavoidable decrease in the internal surface area of the photoelectrode film.

Some recent developments have reported oxide nanocrystallite aggregates for an application in DSCs [2, 10, 48-52]. It was demonstrated that the use of oxide nanocrystallite aggregates might provide the photoelectrode with a large specific surface area and meanwhile efficient light-scattering centers. This has resulted in very impressive enhancements in the overall conversion efficiency for either ZnO or TiO_2-based DSCs. This review introduces the synthesis and characterization of ZnO and TiO_2 aggregates, and shows that the light scattering

effect with these aggregates may significantly enhance the LHE of photoelectrode and thus improve the conversion efficiency of solar cells.

2. PHOTOELECTRODE WITH ZnO AGGREGATE FILM

2.1 Synthesis of ZnO aggregates and preparation of photoelectrode films

ZnO aggregates were synthesized by a hydrolysis of zinc salt in polyol medium along with heating at 160 °C [51, 53]. Typically, zinc acetate dihydrate (0.01 mol) was added to diethylene glycol (DEG, 100 mL) with vigorous stirring. The mixture was rapidly heated in an oil bath at a rate of 10 °C/min. The reaction continued for about 8 h with continual stirring. As-obtained colloidal solution was then sequentially concentrated by 1) centrifugally separating the aggregates from the solvent, 2) removing the supernatant, and 3) redispersing the precipitate in ethanol (5 mL). The sample synthesized at 160 °C is denoted as Sample 1, while three more samples else synthesized at temperatures of 170 °C, 180 °C, and 190 °C are denoted as Samples 2 through 4, respectively.

Photoelectrode films of ~0.5 cm^2 in size were fabricated on FTO glass using a drop-casting method. After the films dried, they were annealed at 350 °C for 1 h to remove any residual organic matter from the ZnO surface. The films were then sensitized by immersing them into 0.5 mm ethanolic solution of the ruthenium complex cis-$[RuL_2(NCS)_2]$ (commercially known as N3 dye) [54, 55] for approximately 20 min. The sensitization time was controlled strictly and limited to avoid the dissolution of surface Zn atoms and the formation of Zn^{2+}/dye complexes, which might block the electron transport from the dye to semiconductor. The films were then rinsed with ethanol to remove the additional dye.

2.2 Characterization of ZnO aggregates

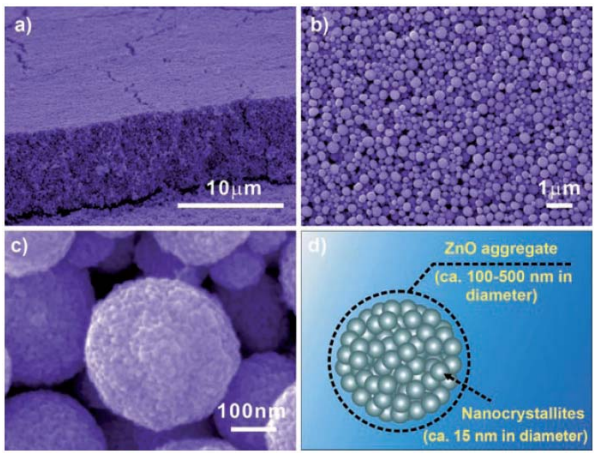

Fig. 1. (a-c) SEM images of ZnO film with aggregates synthesized at 160 °C (Sample 1), and (d) a schematic showing the structure of individual aggregates.

Shown in Fig. 1 are the scanning electron microscope (SEM) images of the film of ZnO aggregates synthesized at 160 °C (Sample 1). It can be seen that the film approximately 10 μm in thickness is well stacked with submicrometer-sized ZnO aggregates. These aggregates

are polydisperse in size with diameters ranging from several tens to several hundreds of nanometers. The film therefore presents a highly disordered structure. The SEM image with a high magnification reveals that the ZnO aggregate is nearly spherical in shape and consists of packed nanocrystallites. In Fig. 1d, the structure of an individual aggregate is schematically illustrated to further demonstrate the porous features provided due to the agglomeration of nanosized crystallites. This ZnO film was thought as a hierarchical structure in view of the architecture formed by secondary submicron-sized aggregates with primary nanocrystallites.

Shown in Fig. 2 are the SEM images of the Samples 2 through 4. It is clear that, with increasing synthesis temperature, the degree of a spherical agglomeration of the nanocrystallites is gradually degraded. The Sample 2, synthesized at 170 °C, is similar to Sample 1 and consists of aggregated ZnO nanocrystallites, but starts to appear a slight destruction in the spherical shape (Fig. 2a). The Sample 3, synthesized at 180 °C, consists of partial aggregates, however most of the aggregates have lost their spherical shape (Fig. 2b). As the synthesis temperature increases further to 190 °C, the obtained product (Sample 4) only presents dispersed nanocrystallites without any agglomeration (Fig. 2c).

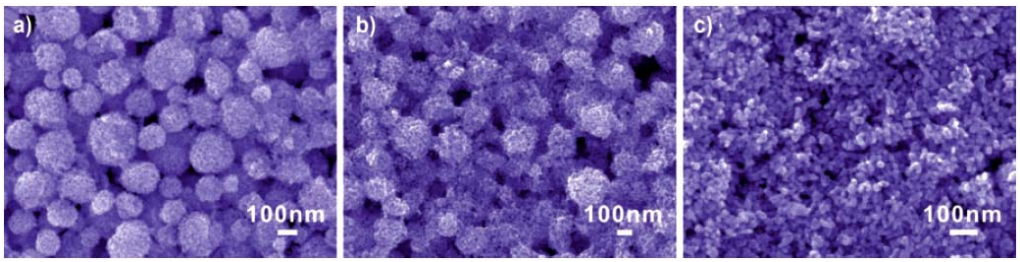

Fig. 2. SEM images of ZnO films with synthesis temperature at (a) 170 °C, (b) 180 °C, and (c) 190 °C, corresponding to Samples 2 through 4, respectively.

X-ray diffraction (XRD) analysis indicated that all the samples were of a hexagonal wurtzite structure of ZnO. With XRD spectra and using the Scherrer equation [56], the primary nanocrystallite size was estimated to be about 15 nm in diameter for all the samples, i.e., there was no appreciable difference in the nanocrystallite size for these samples, despite the differences in synthesis temperature and morphology. Nitrogen sorption isotherms revealed that all four samples possessed almost equal specific surface area of approximately 80 m^2/g.

2.3 Light scattering of ZnO aggregate films

It was observed that Samples 1 through 4, i.e., the ZnO films synthesized at different temperatures, presented an apparent difference in their transparency. This was explained to be a result of light scattering, which reflected on optical absorption spectra of the dye sensitized films, as shown in Fig. 3. In the spectra below 390 nm, all the samples exhibit an intrinsic absorption with similar absorption intensity. This is caused by the ZnO semiconductor owing to electron transfer from the valence band to the conduction band. However, absorption at wavelengths above 400 nm varies significantly; such absorption originates from the dye molecules adsorbed on the ZnO surface and is related to the film structure. It has the highest intensity for Sample 1, less intensity for Samples 2 and 3, and the lowest intensity for Sample 4. It should be noted that only Sample 4 presents an absorption peak centered around 520 nm, corresponding to the visible $t_2 \rightarrow \pi^*$ metal-to-ligand charge transfer (MLCT) [55] in N3 dye but with a slight blue-shift due to the electronic coupling between N3 and ZnO, whereas the

other three samples (1-3) show a monotonically increased absorption as the wavelength switches from visible to ultraviolet. The absorption spectra illustrate that the better aggregation of nanocrystallites induces more effective photon capturing in the visible region and also suggest the existence of a strong light scattering effect. Such an effect may partially scatter the incident light and weaken the transmittance of the films and, thus, result in the pseudo absorption deviating from that of adsorbed dye.

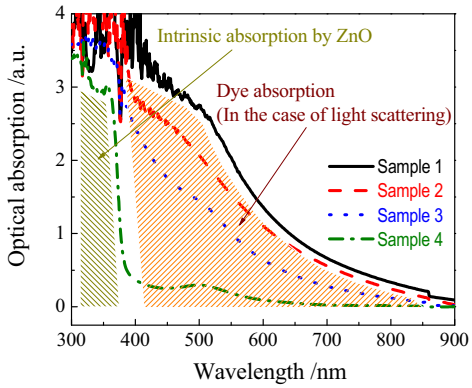

Fig. 3. Comparison of optical absorption spectra of ZnO aggregate films (Samples 1 through 3) and nanocrystallite film (Sample 4).

Lorenz-Mie-Debye theory [57, 58] and Anderson localization of light [59] provide the analytical description for the scattering of light by spherical particles and predict that resonant scattering may occur when the particle size is comparable to the wavelength of incident light. The aggregates within ZnO films are submicrometer-sized, and they are therefore particularly efficient scatterers for visible light, resulting in a significant increase in the light-harvesting capability of the photoelectrode. Unlike large oxide particles, the ZnO aggregates are closely packed with nanocrystallites and therefore do not cause any loss in the internal surface area. It should be noted that the light scattering effect is usually imperceptible in conventional mesoporous TiO_2 electrodes consisting of nanocrystallites smaller than 50 nm, because the size is far away from the wavelength of visible light; this is also the reason that Sample 4 presents a relatively weak absorption at the visible wavelengths.

2.4 Solar cell performance

The solar cells with as-prepared ZnO films were characterized by measuring the current–voltage behavior while the cells were irradiated by simulated AM 1.5 sunlight with a power density of 100 mW/cm^2. Figure 4 shows typical current density versus voltage curves of the four ZnO samples. Sample 1, with near perfect aggregation, achieved the highest short-circuit current density and, thus, the highest conversion efficiency, whereas Sample 4, consisting of only ZnO nanocrystallites, presented the lowest current density and the lowest energy conversion efficiency among all four samples. Table 1 summarizes the open-circuit voltages, the short-circuit current densities, the fill factors, and the overall energy conversion efficiencies for all four samples. All samples possessed the same or similar open-circuit voltages of approximately 600 mV; however, the short-circuit current density varied significantly from 19 mA/cm^2 for Sample 1 to 10 mA/cm^2 for Sample 4. As a result, the

energy conversion efficiency varied systematically from 5.4% for Sample 1 to 2.4% for Sample 4, decreasing as the degree of spherical aggregation decreased.

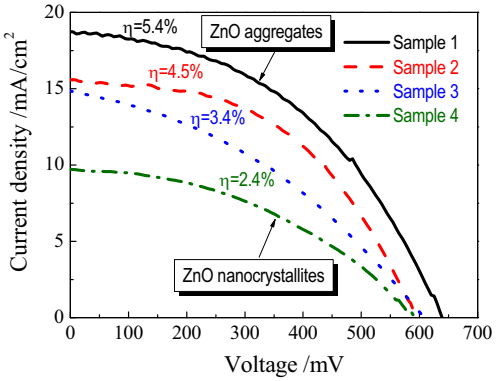

Fig. 4. Photovoltaic response of ZnO aggregate films (Samples 1 through 3) and nanocrystallite film (Sample 4). All samples were irradiated by standard AM 1.5 sunlight with an output power of 100 mW/cm^2.

Table 1. Photovoltaic properties of dye-sensitized ZnO solar cells. (Samples 1 through 3: aggregate films, Sample 4: nanocrystallite film.)

Sample	V_{OC} [mV]	I_{SC} [mA/cm^2]	FF [%][a]	η [%][a]
1	635	18.7	45.1	5.4
2	595	15.6	48.7	4.5
3	605	14.9	37.8	3.4
4	595	9.7	41.1	2.4

[a] The conversion efficiency η and fill factor FF are calculated from $\eta=P_{out,max}/P_{in}$ and $FF= P_{out,max}/(V_{OC}\times I_{SC})$, where $P_{out,max}$ is the maximum output power density, P_{in} is the incident light power density, V_{OC} is the photovoltage at open circuit and I_{SC} is the photocurrent density at short circuit.

In view of different optical absorption of these films, the variation in the solar cell conversion efficiency could be attributed to light scattering generated because of the disordered film structure formed by the polydisperse aggregates. A disordered structure may lead to random multiple scattering in the film and, possibly, result in light localization due to the formation of traps for optical confinement. Photoinduced lasing emission on closely packed ZnO cluster films reported by Cao *et al.* [60] and Wu *et al.* [61] is one example that manifests the light scattering effect of highly disordered structure on the generation of light localization. In ZnO solar cells that consist of a photoelectrode film with aggregates, the light scattering may significantly extend the traveling distance of light within the photoelectrode film and, thus, increase the probability of interaction between the photons and dye molecules. That means, the light scattering may result in an enhancement in the LHE of photoelectrode and therefore increases the conversion efficiency of solar cells. This is just the reason that, in Fig. 4, Sample 1 achieves a conversion efficiency of 5.4%, much higher than 2.4% obtained for Sample 4, the ZnO nanocrystalline film without light scattering.

2.5 Size dependence of conversion efficiency

Size dependence of the solar cell conversion efficiency was investigated to further demonstrate that the light scattering effect was closely related to the structure of the photoelectrode film, such as the average size and size distribution of the aggregates. For this purpose, both monodisperse and polydisperse ZnO aggregates were prepared. The method for the synthesis of polydisperse ZnO aggregates is a polyolmediated precipitation method similar to that described in Sec. 2.1, however the rate of heating was adopted to be different to control the degree of polydispersity. Specifically, a rapid heating at 10 °C/min was used to fabricate the polydisperse ZnO aggregates with a broad size distribution, while a rate of 5 °C/min was used to obtain the polydisperse aggregates with the relatively narrow size distribution. To synthesize monodisperse ZnO aggregates, an amount of stock solution was added into the reaction solution when the temperature reached 130 °C and meanwhile the zinc acetate was completely dissolved. The stock solution was made of 5 nm ZnO nanoparticles prepared via a sol–gel approach and dispersed in the diethylene glycol with a concentration of about 10^{-3} M. The size of the aggregates could be adjusted by the amount of stock solution added to the reaction solution. For example, 0.5 mL, 1 mL, 5 mL, 10mL and 20mL of stock solution were added and attained the monodisperse ZnO aggregates of 350 nm, 300 nm, 250 nm, 210nm and 160nm in diameter, respectively.

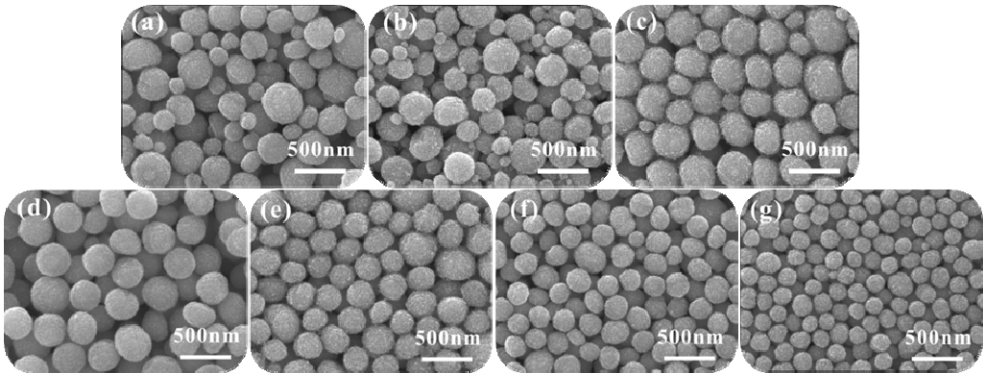

Fig. 5. SEM images of ZnO films with aggregates different in size and size distribution. (a) and (b): Polydisperse aggregates which are different in the polydispersity of the aggregates, corresponding to groups 1 and 2, respectively. (c-g): monodisperse aggregates which are different in the aggregate size, corresponding to groups 3 through 7, respectively.

To study the effects of the average size and size distribution of the aggregates on the solar-cell performance, a number of ZnO films with various structures were prepared and classified into seven groups, named group 1, 2, . . . through 7, in which the films in groups 1 and 2 were made of polydisperse ZnO aggregates and the others only included monodisperse aggregates. Figure 5 shows typical SEM images of all these film samples, where Figures 5(a) through (g) correspond to the samples that belong to groups 1 through 7, respectively. One can see that the samples in group 1 consisted of polydisperse ZnO aggregates with diameter varying from 120 to 360 nm, while the samples in group 2 also consisted of polydisperse ZnO aggregates but with the diameter in the region of ~120-310 nm. The other samples were all monodisperse ZnO aggregates with average sizes varying from ~350 nm for group 3, ~300 nm for group 4, ~250 nm for group 5, ~210 nm for group 6, to ~160 nm for group 7.

The solar-cell performance of all the samples is summarized in Fig. 6, where Fig. 6a shows the dependence of the energy-conversion efficiency on the diameter and size distribution of the aggregates, and Fig. 6b indicates a similar trend for the short-circuit current density. It is clear that the photoelectrode films with polydisperse ZnO aggregates have both a higher energy-conversion efficiency and a larger short-circuit current density than the films with monodisperse ZnO aggregates. To speak in detail, the electrode films consisting of polydisperse ZnO aggregates with a maximum diameter of 360 nm (samples in group 1) present the highest conversion efficiency of all the samples of 4.4%, approximately 33% higher than the efficiency of 3.3% achieved for the polydisperse ZnO aggregates with the maximum diameter of 310 nm (samples in group 2), and 63% higher than the efficiency of 2.7% for the monodisperse ZnO aggregates with an average size of ~350 nm (samples in group 3). Similarly, the largest short-circuit current density of 21 mA/cm^2, achieved for the polydisperse ZnO aggregates with the maximum diameter of 360 nm (samples in group 1), is 40% higher than that of 15 mA/cm^2 for the polydisperse ZnO aggregates with the maximum diameter of 310 nm (samples in group 2), and 75% higher than that of 12 mA/cm^2 for the monodisperse ZnO aggregate films (samples in group 3). As for the ZnO films with only monodisperse aggregates, one can see that the decrease in the size of the ZnO aggregates directly results in the degradation of the short-circuit current density from 12 mA/cm^2 to 7 mA/cm^2 and the energy-conversion efficiency from 2.7% to 1.5%. It has been demonstrated that the variation of conversion efficiency for the ZnO solar cell samples in different groups only results from the difference in photocurrent of the cells instead of open-circuit voltage or fill factor. Moreover, the photocurrent was basically related to either the dye adsorption amount determined by the internal surface area of the photoelectrode film or the propagation behavior of light within the photoelectrode film. However, a nitrogen sorption isotherm measurement revealed a same specific surface area, ~80 m^2/g, for all these samples in different groups. For this reason, the dye adsorption amount was thought unlikely to be the reason that causes the difference in the short-circuit current density. Therefore, it was inferred that the film structures with differences in the aggregate size and size distribution might lead to different impacts on the transport of light so that the LHE of the photoelectrode was significantly affected.

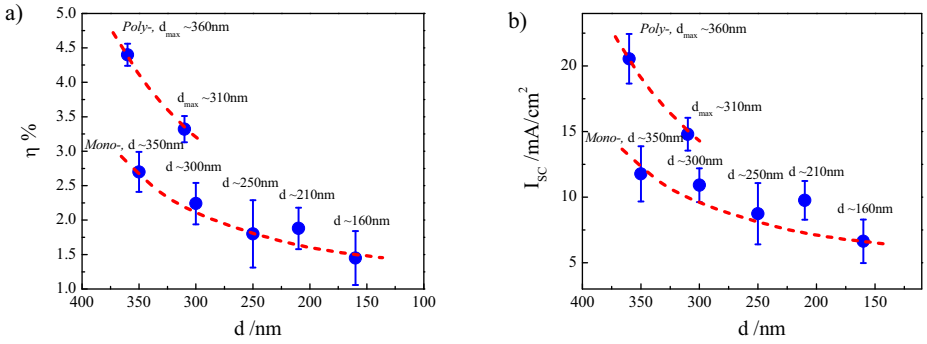

Fig. 6. Dependence of (a) overall DSC conversion efficiency and (b) short-circuit current density on the geometrical structure of the films consisting of ZnO aggregates different in size or size distribution.

To demonstrate the impact of film structure on the transport of light, optical absorption spectra of all the films in seven groups were measured, as shown in Fig. 7. The film with 160-nm diameter ZnO nanocrystallites presented a typical absorption like that obtained for single

crystalline ZnO. The absorption below 385 nm, corresponding to the band gap energy of 3.2 eV, represents the intrinsic optical absorption of ZnO semiconductor caused by the electron transit from the valence band to the conduction band. Almost no absorption can be observed from this film in the visible region with wavelength above 385 nm. As the ZnO aggregates of nanocrystallites are gradually formed and the aggregate size becomes increased, the optical absorption of films in the visible region is apparently increased. The most significant increase occurs on the film that belongs to group 1 consisting of polydisperse ZnO aggregates with a broad size distribution from 120 to 360 nm in diameter. The result implies that the enhancement in optical absorption originates from the aggregation of ZnO nanocrystallites and is proportional to the average size of mono-sized aggregates or the dispersion degree of polydisperse aggregates in size distribution. This phenomenon can be explained by the light scattering of submicron-sized ZnO aggregates, which may change the transport direction of light travelled in the films and hereby attenuate the light that transmits through the films.

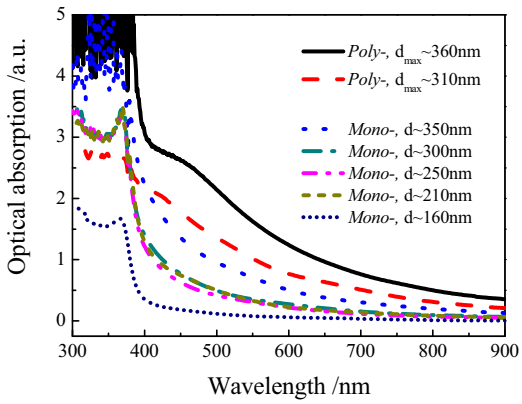

Fig. 7. Optical absorption spectra of ZnO films consisting of aggregates with different sizes and size distributions.

Light scattering by spherical particles can be analytically described by the Lorenz-Mie-Debye resonance theory, in which the scattering efficiency, Q_{sca}, is given by [62, 63]

$$Q_{sca} = \frac{2}{x^2}\sum_{n=1}^{\infty}(2n+1)(|a_n|^2 + |b_n|^2), \tag{1}$$

where $x = 2\pi r/\lambda$ is the size parameter, r is the radius of dielectric sphere, λ is the wavelength of light, a_n and b_n are the complex Mie coefficients that can be calculated as

$$a_n = \frac{\psi_n'(mx)\psi_n(x) - m\psi_n(mx)\psi_n'(x)}{\psi_n'(mx)\zeta_n(x) - m\psi_n(mx)\zeta_n'(x)}, \tag{2}$$

$$b_n = \frac{m\psi_n'(mx)\psi_n(x) - \psi_n(mx)\psi_n'(x)}{m\psi_n'(mx)\zeta_n(x) - \psi_n(mx)\zeta_n'(x)} \tag{3}$$

where m is the refractive index of dielectric sphere, ψ and ζ are the Riccati-Bessel functions [64, 65]. Figure 8 presents the results on a calculation of the scattering efficiency for mono-

sized ZnO aggregates with the diameter varied from 160 nm to 350 nm, corresponding to the samples in groups 3 through 7. During the calculation, the wavelength-dependent refractive index of ZnO was obtained from the literature [66]. From Fig. 8, one can see that the scattering efficiency is a function of incident wavelength and aggregate size. In the wavelength range of 400 ~ 900 nm, and statistically, the sample consisting of large aggregates with 350 nm diameter possesses the largest scattering efficiency, whereas the sample with 160 nm aggregates has the lowest scattering efficiency. This is reasonable because a resonant scattering most likely occurs when the size of aggregates is comparable with the wavelength of incident light. The calculated results of optical scattering efficiency for mono-sized aggregates as presented in Fig. 8 show a trend that the scattering becomes more intensive as the aggregate size increases. This verifies that the absorption enhancement reflecting on the experimental absorption spectra for larger sized aggregates is a result of light scattering.

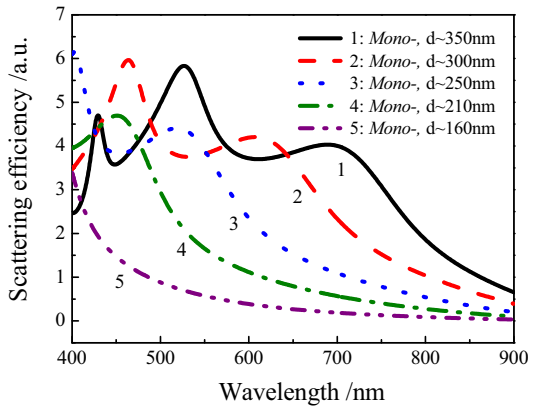

Fig. 8. Theoretical light scattering efficiency as a function of the wavelength while the scatterer size is changed in a range from 160 nm to 350 nm.

The light scattering influences the transport behavior of light through changing the path and/or extending the distance of light travelled within the photoelectrode film. As a result, the light harvesting efficiency gets improved due to the increased probability of interaction between the photons and the dye molecules that adsorb on the ZnO nanocrystallites. Compared with the films that contain only mono-sized aggregates, the films with polydisperse aggregates take an apparent advantage in the enhancement of optical absorption and energy conversion efficiency, as shown in Figures 7 and 6a, respectively. Polydisperse aggregates likely lead to disordered structure when they are packed in a random way to form the film. Many literatures have demonstrated that the less ordered medium is more effective in the generation of multiple scattering to light and the formation of closed loops for light confinement [60, 61, 67]. The broader distribution of aggregate size means the increased irregularity in the assembly of film, resulting in the fact that, as mentioned above, the samples in group 1 consisting of polydisperse aggregates with the size distribution in a quite large range possess the highest conversion efficiency. Another reason that polydisperse aggregates exhibit excellent ability on the enhancement of optical absorption as well as solar cell efficiency is the different sized aggregates that can cause the light scattering in a wide wavelength range. Besides the generation of light scattering effect, the polydisperse aggregates are also thought to be of benefit to forming network interconnection and creating the photoelectrode film with a closely-packed structure, which may offer more pathways for the transport of electrons within the film.

2.6 Lithium ions induced improvement in solar cell performance

As an attempt to optimize the morphology and the surface chemistry of the aggregates, lithium ions were employed to mediate the growth of the ZnO aggregates. Such an approach has been proved to be effective in the increase of both the nanocrystallite size and the polydispersity of the aggregate size. This leads to improved dye adsorption and more effective light scattering for the photoelectrode film. An almost 53% increase in the conversion efficiency has been reported for the ZnO aggregates synthesized in the presence of lithium ions [52].

The fabrication of ZnO aggregates is similar to what is described in Sec. 2.1 but lithium ions are utilized to mediate the growth of the aggregates. For a typical fabrication process, 0.1 M zinc acetate dihydrate ($ZnAc \cdot 2H_2O$) and 0.01 M lithium salt (e.g. $LiAc \cdot 2H_2O$) were added to diethylene glycol (DEG) and the mixture was heated to 160 °C at a rate of 5 °C/min. The solution was kept at 160 °C for about 2 h so as to allow for the necessary chemical reactions to occur. Same as a treatment for preparing pure ZnO aggregates, the colloid was then concentrated by a sequential treatment of centrifugation, removal of the supernatant, and several redispersals of the precipitate in ethanol. The precipitate was finally dispersed in ethanol with a concentration of approximately 0.5 M and as-obtained colloidal suspension solution was ready for making photoelectrode film. The ZnO aggregates synthesized in the presence of lithium ions was denoted as "Li-ZnO". For comparison, "pure-ZnO" aggregate films were also prepared as reference while the reaction solution only contained $ZnAc \cdot 2H_2O$ and DEG.

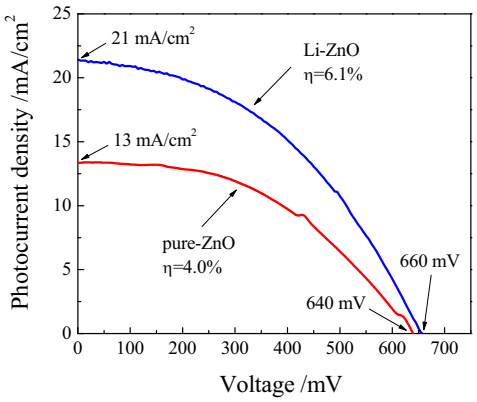

Fig. 9. Photovoltaic behavior of ZnO films consisting of aggregates synthesized in the presence (denoted as "Li-ZnO") and absence (denoted as "pure-ZnO") of lithium ions.

Figure 9 shows the typical photovoltaic behavior of ZnO films consisting of aggregates synthesized in the presence and absence of lithium ions. These two types of films display similar open-circuit voltages (V_{OC}) in the range of 640-660 mV and fill factors (FF) of 0.44-0.48. However, they differ in short-circuit photocurrent densities (I_{SC}), i.e., 13 mA/cm^2 for pure-ZnO and 21 mA/cm^2 for Li-ZnO. The larger photocurrent density leads to higher conversion efficiency. The efficiency of the Li-ZnO film reached 6.1%, while a value of 4.0% was attained for the pure-ZnO film. Such a significant enhancement in the conversion efficiency was ascribed to the use of lithium ions during the ZnO aggregate synthesis, which offered a positive influence on the solar cell performance by affecting the morphology,

structure, and surface chemistry of the aggregates, and thus resulted in increased dye adsorption and more effective light scattering.

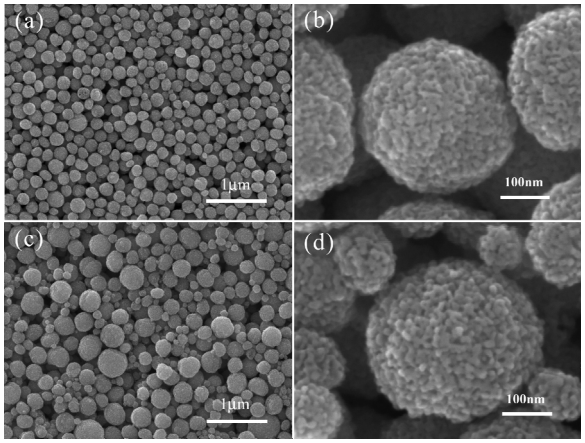

Fig. 10. SEM images of the films with (a, b) pure-ZnO and (c, d) Li-ZnO aggregates.

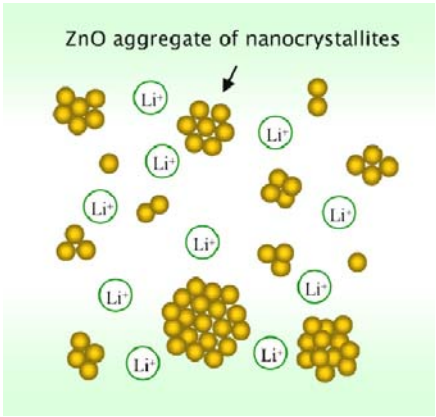

Fig. 11. A schematic showing the impact of lithium ions on the growth of ZnO aggregates.

Shown in Fig. 10 are the SEM images of pure-ZnO and Li-ZnO films. An apparent difference in the morphology can be seen under low magnification (Figures 10a and c). The pure-ZnO film is comprised of aggregates with a monodisperse size distribution, whereas the Li-ZnO film exhibits a broad distribution of aggregate size from several tens to several hundreds of nanometers. The different polydispersity of ZnO aggregates synthesized in the presence of lithium salt reflects the important influence of lithium ions on the growth of ZnO aggregates. As the schematic drawing shown in Fig. 11, it is possible that these lithium ions adsorb on the ZnO surface so as to mediate the agglomeration of ZnO nanocrystallites. A polydisperse size distribution of Li-ZnO aggregates is beneficial to light scattering, and it was

thought to contribute to the light harvesting efficiency of the photoelectrode and partially resulted in an increase in the conversion efficiency of the cells.

The difference of pure-ZnO and Li-ZnO films in the light scattering ability was confirmed by measuring optical absorption spectra of these two films. The results are shown in Fig. 12. It can be seen that both of these films present an intrinsic absorption band at wavelengths below 385 nm and an additional absorption hump in the visible region. The latter is thought to be a result of light scattering, which causes light extinction via diffuse reflection and/or diffuse transmission. This affects the film transparency and appears in the spectra as pseudo-absorption. For the Li-ZnO film, it shows that the absorption in the visible region is stronger than that of the pure-ZnO. This is just because the aggregates in the Li-ZnO film are highly polydisperse in size and may generate more efficient light scattering than the monodisperse aggregates.

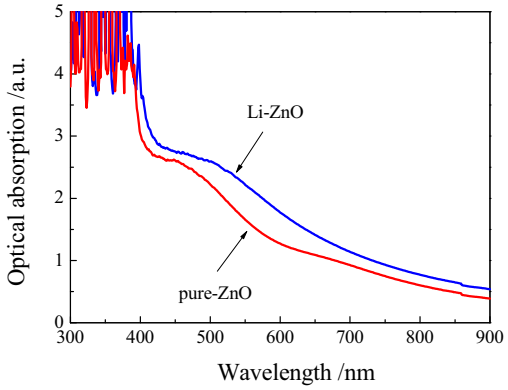

Fig. 12. Optical absorption spectra of pure-ZnO and Li-ZnO films.

Besides enhanced light scattering effect due to the polydispersity of ZnO aggregates in size, the use of lithium ions in the synthesis was also mentioned to increase the nanocrystallite size of ZnO and the pore size of aggregates. This offered a more porous structure for dye infiltration and electrolyte diffusion. Furthermore, the presence of lithium ions might else enhance the surface stability of ZnO, which prevented the formation of Zn^{2+}/dye complexes and favored dye adsorption on ZnO in a monolayer. All these factors were thought to jointly improve the solar cell performance. It is worth addressing that these samples were characterized through X-ray photoelectron spectroscopy (XPS). However, no detectable difference could be found in the XPS spectra for the pure-ZnO and Li-ZnO films, indicating that these two films are identical with regards to chemical composition. In other words, it excludes the possibility that lithium exists in the ZnO as a dopant or forms a composite with ZnO, although the term "Li-ZnO" is used to represent the ZnO aggregates that are synthesized in the presence of lithium ions. The impact of lithium ions on the surface chemistry of ZnO can be else perceived by view of the large short-circuit photocurrent density, 21 mA/cm^2, for Li-ZnO (Fig. 9). To some extent, this means that the absorption onset of the photoelectrode film has been significantly extended to be longer than ~750-nm wavelength, which is the near-infrared absorption edge of the N3 dye [68]. Such a scenario can be suggested to be a result of an enhancement in the coupling between the dye molecules and ZnO semiconductor, which contributes to the light absorption in the long wavelength region [52].

3. TiO_2 AGGREGATES AS LIGHT SCATTERING CENTERS

3.1 Synthesis of TiO_2 aggregates and characterization of photoelectrode films

With an attempt of following the same strategy as ZnO aggregates for light scattering, TiO_2 aggregates were also synthesized and studied on their photovoltaic performance. The synthesis of the TiO_2 aggregates was carried out by first fabricating TiO_2 spheres through adding a mixture of 1 mL of titanium isopropoxide and 30 mL of ethylene glycol into 400 mL of acetone containing 1 mL of DI-water under vigorous stirring [69]. The precipitate of TiO_2 spheres was then treated with 500 mL of DI-water containing 0.5 mL of acetate acid in a reflux at 120 °C for 1.5 h. This step leads to the formation of nanocrystallite aggregates. The product was then washed with ethanol several times, dried at 100 °C, and finally ground into a fine powder for use. With a TiO_2 sol and using a hydrothermal method [70, 71], nanocrystalline TiO_2 was also synthesized and mixed with TiO_2 aggregates in a given ratio to form different structured photoelectrode films. Sample *I* consists of TiO_2 nanocrystallites alone. Sample *II* is made of only TiO_2 aggregates. Samples *III* through *V* are films of nanocrystallites admixed with aggregates in different ratios: 3:1 (nanocrystallites:aggregates in weight) for Sample *III*, 1:1 for Sample *IV*, and 1:3 for Sample *V*. All films of ~0.25 cm^2 in size were prepared to be approximately 10 μm in thickness, annealed at 450 °C for 30 min, and sensitized with 0.5 mM N719 dye ($[RuL_2(NCS)_2]$:2TBA, TBA=tetra-n-butylammonium).

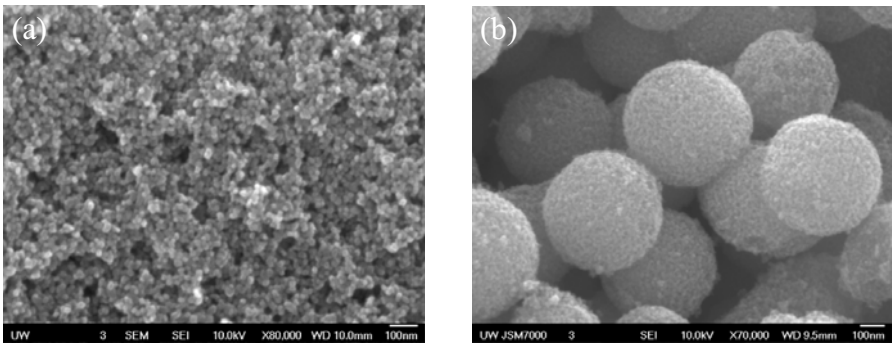

Fig. 13. SEM images of (a) a TiO_2 nanocrystalline film (Sample *I*) and (b) a TiO_2 aggregate film (Sample *II*).

Shown in Fig. 13 are the SEM images of Sample *I* (the TiO_2 nanocrystalline film) and Sample *II* (the TiO_2 aggregate film). It can be seen that Sample *I* is formed by disperse nanocrystallites with an average diameter of about 20 nm. This structure is the same as those used for photoelectrode films in traditional DSCs fabricated with P25 powder (Degussa, Germany). Sample *II* is composed of spherical TiO_2 aggregates with submicron dimensions. A very rough surface can be observed for the aggregates in Sample *II*. This is thought to be the result of the porous structure of the aggregates. With a TEM observation, it has been revealed that the aggregates are comprised of interconnected nano-sized crystallites [72, 73]. The porosity of the as-synthesized aggregates was also evident through characterization of the specific surface area using the BET (Brunauer-Emmett-Teller) technique [74]. A value of ~100 m^2/g was attained for the aggregates.

Shown in Fig. 14 are the XRD patterns of Sample *I* and Sample *II*. It can be seen that the film of Sample *I*, which consists of nanocrystalline TiO_2, possesses a pure anatase crystal structure. However, the film of Sample *II*, which is comprised of aggregates, contains anatase

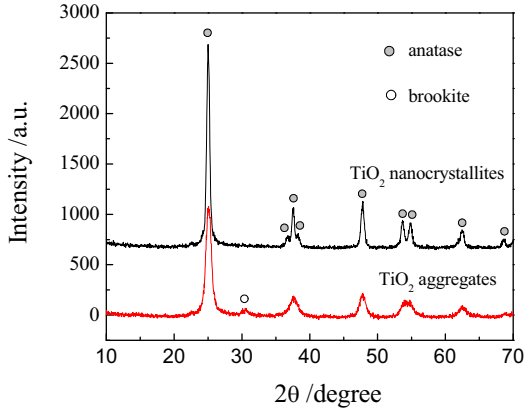

Fig. 14. XRD patterns of TiO_2 nanocrystalline film and aggregate film.

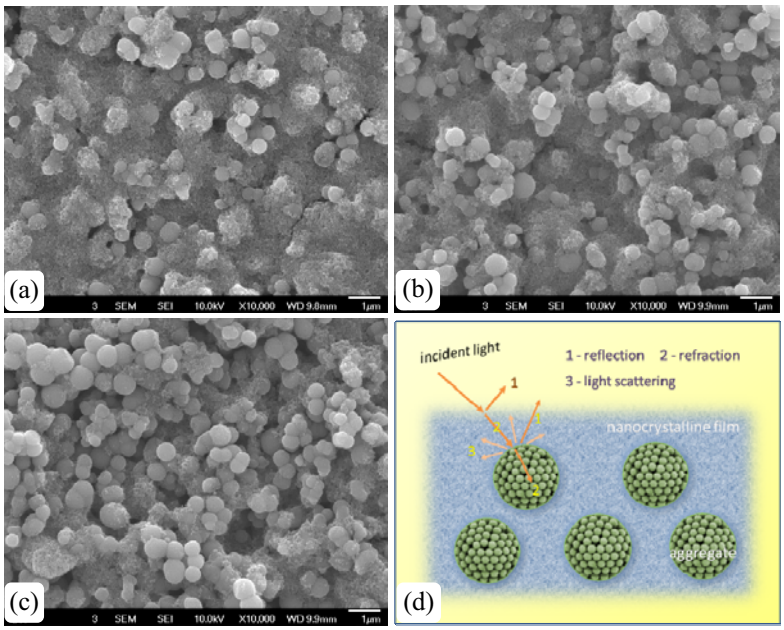

Fig. 15. SEM images of films consisting of nanocrystallites admixed with aggregates in a ratio of (a) 3:1 (Sample *III*), (b) 1:1 (Sample *IV*), and (c) 1:3 (Sample *V*). The schematic in (d) shows the embedded structure of TiO_2 aggregates in the nanocrystalline film and the generation of light scattering.

and a small fraction of brookite. In DSCs with a TiO_2 photoelectrode film, it is well-known that the solar cell performance is crucially dependent on the TiO_2 crystal structure. This is because the crystal structure affects both the adsorption density of dye molecules on the TiO_2 and the injection efficiency of electrons transferring from the dye to the TiO_2 semiconductor. Compared to the rutile and brookite phases, anatase TiO_2 has been proven to be the preferred phase for achieving high density dye adsorption and efficient electron injection [75]. The

difference in the crystal structures of Samples *I* and *II* results from the use of different synthesis routes, i.e., hydrothermal growth for the nanocrystalline TiO_2 and hydrolysis fabrication at a relatively low temperature for the aggregates. Based on the XRD patterns shown in Fig. 14, the average crystallite sizes were estimated to be ~18 nm for Sample *I* (the nanocrystalline film) and ~8 nm for Sample *II* (the aggregate film). The latter reflects the size of nanocrystallites that form into the aggregates.

Samples *III* through *V* are hybrid films consisting of nanocrystallites and aggregates in three different ratios (nanocrystallites:aggregates in weight), 3:1 for Sample *III*, 1:1 for Sample *IV*, and 1:3 for Sample *V*. Shown in Fig. 15 are the SEM images of these samples. It is evident that the submicron aggregates and the nanoscale crystallites are homogeneously blended. This ensures uniform scattering of the light within the nanocrystalline films. Shown in Fig. 15(d) is a schematic diagram demonstrating the embedded structure of the hybrid films. The TiO_2 aggregates act as light scatterers and, thus, cause the light to travel through a much longer distance within the film when compared to the case of no light scattering. Since the crystallite size of the nanocrystalline film is far smaller than the wavelength of visible light, light in the film propagates in a straight direction, penetrates through, and ultimately, with the exception of the light being absorbed, moves away from the film.

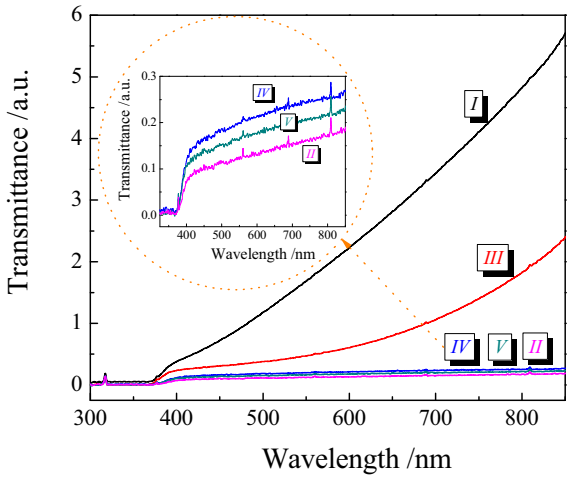

Fig. 16. A comparison of the optical transmittance of the TiO_2 nanocrystalline film (Sample *I*), aggregate film (Sample *II*), and the films of nanocrystallites mixed with aggregates in different ratios: 3:1 (Sample *III*), 1:1 (Sample *IV*), and 1:3 (Sample *V*). The inset shows a magnified view of the spectra of Samples *II*, *V*, and *IV*.

The existence of light scattering caused by aggregates in the films of Samples *II* through *V* can be noted by simply observing the transparency and the film color. For example, Sample *I* (the nanocrystalline film with no aggregates) is almost transparent, even though it is almost 10 μm in thickness. However, Sample *II* (the aggregate film with the same thickness) is a milky white color and has an extremely low transparency. As shown in Fig. 16, the difference in the transparency can be reflected experimentally by comparing the transmittance of the films. Among the films, it can be seen that Sample *I* (the nanocrystalline film) exhibits the highest transmittance. This is because the size of the nanocrystallites in Sample *I* is far smaller than the wavelength of visible light. With the exception of the light that is being absorbed, most of the incident light with a photon energy larger than the band gap of TiO_2

(~3.2 eV) can pass through the film and be detected as a transmitted portion. Sample *II* (the film consisting of aggregates) presents the poorest transmittance. This arises from the light scattering generated by the aggregates. As stated above, the aggregates possess a submicron size that is comparable to the wavelength of visible light. As such, incident light is efficiently scattered. This results in an extinction of the light that transmits through the film. The films of Samples *III* through *V*, which are composed of nanocrystallites and aggregates, show transmittance intensities between those of Sample *I* and Sample *II*. As the ratio of aggregates to nanocrystallites is increased, the intensities of the film transmittance gradually decrease.

3.2 Increased solar cell efficiency with TiO_2 aggregate scatterers

Photovoltaic performance of Samples *I* through *V* is summarized in Table 2. It is evident that the hybrid films and the films of nanocrystallites and aggregates exhibit an apparent difference in the overall solar cell conversion efficiency even though the film fabrication, dye sensitization, and solar cell assembly process were the same for all samples. While Sample *I*, the nanocrystalline film, yielded an intermediate efficiency of 5.6%, the highest conversion efficiency, 6.8%, was achieved on Sample *IV*, the nanocrystalline film composed of 50% aggregates. In other words, when aggregates were employed as scatterers, an almost 21% increase in the conversion efficiency was attained. In Samples *III* (25% aggregates) and *V* (75% aggregates), the conversion efficiency decreased to 5.5% and 5.0%, respectively. This result implies that the enhancement effect on the conversion efficiency can be only achieved when the nanocrystallites are mixed with the aggregates in a certain ratio, for example, ~50% in this study. Such a scenario can be explained by a decrease in amount of dye adsorbed on the photoelectrode films due to the unsuitable surface facets of the nanocrystallites that form into the aggregates. This counteracts the light scattering effect. Therefore, an enhancement in the conversion efficiency can only be achieved when the content of aggregates in nanocrystalline film is within a proper percentage.

Table 2. Summary of the open-circuit voltage (V_{OC}), short-circuit current density (I_{SC}), maximum voltage (V_{max}) and current (I_{max}) output, fill factor (FF), and overall conversion efficiency (η) relative to the film structure of Samples *I* through *V*.

Sample No.	Description	V_{OC} (mV)	I_{SC} (mA/cm^2)	V_{max} (mV)	I_{max} (mA/cm^2)	FF (%)	η (%)
I	nanocrystallites	710	12.01	535	10.53	66	5.6
II	aggregates	695	8.30	490	5.74	49	2.8
III	25% of aggregates	700	14.60	470	11.70	54	5.5
IV	50% of aggregates	710	14.43	545	12.54	67	6.8
V	75% of aggregates	690	11.19	520	9.55	64	5.0

The unsuitability of the facets of the TiO_2 aggregates can, to some extent, be shown by the XRD patterns of Fig. 14. As mentioned above, Sample *II* contains a small fraction of brookite in addition to anatase. This indicates a difference in the facets between Sample *II* and Sample *I*; the latter is hydrothermally synthesized and is composed of pure anatase phase. While the use of aggregates in a nanocrystalline film may improve the light harvesting by generating light scattering, the unsuitable facets of the aggregates may simultaneously give rise to insufficient dye adsorption and thus, impair the optical absorption of the photoelectrode film. The existence of unsuitable facets would explain the low conversion efficiency of ~2.8% for Sample *II*, which consists of aggregates alone.

Besides the unsuitable facets, an undesirably small pore size of the aggregates as shown in Fig. 13b is also thought to be one of the factors that induce the poor conversion efficiency in the aggregate film (Sample *II*). Such a small pore size is believed to be a bottleneck that may hinder both the infiltration of dye molecules into the aggregates and the diffusion of liquid electrolyte when the solar cell is under an operating condition. In addition, for Sample *II* consisting of aggregates alone, the loosely organized packing structure of the film, which results from the relatively large size of as-made aggregates, would inevitably cause a loss in the surface area of the photoelectrode film. Such a morphology also has the tendency to lower the dye adsorption amount and depress the overall conversion efficiency of the cells.

Obviously, the use of TiO_2 aggregates as light scatterers combined with nanocrystalline film in DSCs is effective for an enhancement in the conversion efficiencies. However, the TiO_2 aggregates synthesized with the method presented in Sec. 3.1 are still non-ideal in the crystal structure and the porosity. Such issues present many opportunities for future work. By developing TiO_2 aggregates to 1) possess proper facets so as to achieve sufficient dye adsorption, and 2) have a more porous structure with a large pore size so as to facilitate dye infiltration and electrolyte diffusion, it is anticipated that the light scattering enhancement effect of the TiO_2 aggregates could be further improved. This would ultimately lead to more significant increase in the conversion efficiencies of dye-sensitized nanocrystalline solar cells.

4. CONCLUSIONS

Oxide nanocrystallite aggregates possess both large specific surface area and suitable size comparable to the wavelength of light. The oxide nanocrystallite aggregates are therefore a class of effective light scatterers and, while used for dye-sensitized solar cells, can generate light scattering and thus extend the traveling distance of light within the photoelectrode film. Such an extension in the light traveling distance may result in an enhancement in the light harvesting efficiency of the photoelectrode and, ultimately, improve the power conversion efficiency of the solar cell.

When this notion was applied to ZnO DSCs, it had been observed a more than 120% increase in the conversion efficiency with photoelectrode film consisting of ZnO nanocrystallite aggregates compared with that comprised of nanocrystallites only. In the case of TiO_2, the photoelectrode film that was formed by TiO_2 aggregates presented pretty poor conversion efficiency much lower than that obtained for nanocrystalline film. This had been attributed to the non-ideal porosity of the TiO_2 aggregates and the unsuitable facets of the nanocrystallites that formed to the aggregates. However, a 21% improvement in the conversion efficiency was still observed for the TiO_2 films made of nanocrystallites mixed with 50% aggregates, indicating the effectiveness of the TiO_2 aggregates as light scatterers in dye-sensitized solar cells. Further optimization of the structure and the surface chemistry of the TiO_2 aggregates, aiming to more significant improvement in the conversion efficiency of dye-sensitized solar cells, is necessary.

Acknowledgements

This work is supported by the U.S. Department of Energy, Office of Basic Energy Sciences, Division of Materials and Engineering under Award No. DE-FG02-07ER46467 (Q.F.Z.), the Air Force Office of Scientific Research (AFOSR-MURI, FA9550-06-1-0326) (K.S.P.), the University of Washington TGIF grant, the Washington Research Foundation, and the Intel Corporation.

References

[1] A. Goetzberger, C. Hebling, and H. W. Schock, "Photovoltaic materials, history, status and outlook," *Mater. Sci. Eng. R* **40**, 1-46 (2003) [doi:10.1016/S0927-796X(02)00092-X].

[2] J. Liu, G. Z. Cao, Z. Yang, D. Wang, D. Dubois, X. Zhou, G. L. Graff, L. R. Pederson, and J.-G. Zhang, "Oriented nanostructures for energy conversion and storage," *ChemSusChem* **1**, p. 22 (2008) [doi: 10.1002/cssc.200800087].

[3] D. M. Bagnall and M. Boreland, "Photovoltaic technologies," *Energy Policy* **36**, 4390-4396 (2008) [doi:10.1016/j.enpol.2008.09.070].

[4] M. Afzaal and P. O'Brien, "Recent developments in II-VI and III-VI semiconductors and their applications in solar cells," *J. Mater. Chem.* **16**, 1597-1602 (2006) [doi:10.1039/b512182e].

[5] R. B. Bergmann, "Crystalline Si thin-film solar cells: a review," *Appl. Phys. A* **69**, 187-194 (1999).

[6] R. Singh, "Why silicon is and will remain the dominant photovoltaic material," *J. Nanophoton.* **3**, 032503 (2009) [doi: 10.1117/1.3196882].

[7] A. Shah, P. Torres, R. Tscharner, N. Wyrsch, and H. Keppner, "Photovoltaic technology: The case for thin-film solar cells," *Science* **285**, 692-698 (1999) [doi:10.1126/science.285.5428.692].

[8] J. S. Ward, K. Ramanathan, F. S. Hasoon, T. J. Coutts, J. Keane, M. A. Contreras, T. Moriarty, and R. Noufi, "A 21.5% efficient Cu(In,Ga)Se-2 thin-film concentrator solar cell," *Prog. Photovoltaics* **10**, 41-46 (2002) [doi:10.1002/pip.424].

[9] J. Yang, A. Banerjee, and S. Guha, "Amorphous silicon based photovoltaics – from earth to the "final frontier"," *Sol. Energy Mater. Sol. Cells* **78**, 597-612 (2003) [doi:10.1016/S0927-0248(02)00453-1].

[10] Q. F. Zhang, C. S. Dandeneau, X. Y. Zhou, and G. Z. Cao, "ZnO nanostructures for dye-sensitized solar cells," *Adv. Mater.* **21**, 4087-4108 (2009) [doi:10.1002/adma.200803827].

[11] J. Bisquert, D. Cahen, G. Hodes, S. Ruhle, and A. Zaban, "Physical chemical principles of photovoltaic conversion with nanoparticulate, mesoporous dye-sensitized solar cells," *J. Phys. Chem. B* **108**, 8106-8118 (2004) [doi:10.1021/jp0359283].

[12] M. Gratzel, "Photoelectrochemical cells," *Nature* **414**, 338-344 (2001) [doi:10.1038/35104607].

[13] J. M. Kroon, N. J. Bakker, H. J. P. Smit, P. Liska, K. R. Thampi, P. Wang, S. M. Zakeeruddin, M. Gratzel, A. Hinsch, S. Hore, U. Wurfel, R. Sastrawan, J. R. Durrant, E. Palomares, H. Pettersson, T. Gruszecki, J. Walter, K. Skupien, and G. E. Tulloch, "Nanocrystalline dye-sensitized solar cells having maximum performance," *Prog. Photovoltaics* **15**, 1-18 (2007) [doi:10.1002/pip.707].

[14] C. Longo and M. A. De Paoli, "Dye-sensitized solar cells: A successful combination of materials," *J. Braz. Chem. Soc.* **14**, 889-901 (2003) [doi:10.1590/S0103-50532003000600005].

[15] H. J. Snaith, "Estimating the Maximum Attainable Efficiency in Dye-Sensitized Solar Cells," *Adv. Funct. Mater.* **20,** 13-19 (2010) [doi:10.1002/adfm.200901476].

[16] M. Gratzel, "Solar energy conversion by dye-sensitized photovoltaic cells," *Inorg. Chem.* **44**, 6841-6851 (2005) [doi:10.1021/ic0508371].

[17] S. Y. Huang, G. Schlichthorl, A. J. Nozik, M. Gratzel, and A. J. Frank, "Charge recombination in dye-sensitized nanocrystalline TiO_2 solar cells," *J. Phys. Chem. B* **101**, 2576-2582 (1997) [doi:10.1021/jp962377q].

[18] C. J. Barbe, F. Arendse, P. Comte, M. Jirousek, F. Lenzmann, V. Shklover, and M. Gratzel, "Nanocrystalline titanium oxide electrodes for photovoltaic applications," *J. Am. Ceram. Soc.* **80**, 3157-3171 (1997).

[19] M. Gratzel, "Conversion of sunlight to electric power by nanocrystalline dye-sensitized solar cells," *J. Photochem. Photobiol. A* **164**, 3-14 (2004) [doi:10.1016/j.jphotochem.2004.02.023].
[20] A. Hagfeldt and M. Gratzel, "Molecular photovoltaics," *Acc. Chem. Res.* **33**, 269-277 (2000) [doi:10.1021/ar980112j].
[21] F. Gao, Y. Wang, D. Shi, J. Zhang, M. K. Wang, X. Y. Jing, R. Humphry-Baker, P. Wang, S. M. Zakeeruddin, and M. Gratzel, "Enhance the optical absorptivity of nanocrystalline TiO_2 film with high molar extinction coefficient ruthenium sensitizers for high performance dye-sensitized solar cells," *J. Am. Chem. Soc.* **130**, 10720-10728 (2008) [doi:10.1021/ja801942j].
[22] M. K. Nazeeruddin, C. Klein, P. Liska, and M. Gratzel, "Synthesis of novel ruthenium sensitizers and their application in dye-sensitized solar cells," *Coord. Chem. Rev.* **249**, 1460-1467 (2005) [doi:10.1016/j.ccr.2005.03.025].
[23] S. Kim, J. K. Lee, S. O. Kang, J. Ko, J. H. Yum, S. Fantacci, F. De Angelis, D. Di Censo, M. K. Nazeeruddin, and M. Gratzel, "Molecular engineering of organic sensitizers for solar cell applications," *J. Am. Chem. Soc.* **128**, 16701-16707 (2006) [doi:10.1021/ja066376f].
[24] J. Ferber and J. Luther, "Computer simulations of light scattering and absorption in dye-sensitized solar cells," *Sol. Energy Mater. Sol. Cells* **54**, 265-275 (1998) [doi:10.1016/S0927-0248(98)00078-6].
[25] A. Usami, "Theoretical study of application of multiple scattering of light to a dye-sensitized nanocrystalline photoelectrochemical cell," *Chem. Phys. Lett.* **277**, 105-108 (1997) [doi:10.1016/S0009-2614(97)00878-6].
[26] S. H. Kang, J. Y. Kim, H. S. Kim, H. D. Koh, J. S. Lee, and Y. E. Sung, "Influence of light scattering particles in the TiO_2 photoelectrode for solid-state dye-sensitized solar cell," *J. Photochem. Photobiol. A* **200**, 294-300 (2008) [doi: 10.1016/j.jphotochem.2008.08.010].
[27] V. Suryanarayanan, K. M. Lee, J. G. Chen, and K. C. Ho, "High performance dye-sensitized solar cells containing 1-methyl-3-propyl imidazolinium iodide-effect of additives and solvents," *J. Electroanal. Chem.* **633**, 146-152 (2009) [doi:10.1016/j.jelechem.2009.05.005].
[28] Z. S. Wang, H. Kawauchi, T. Kashima, and H. Arakawa, "Significant influence of TiO_2 photoelectrode morphology on the energy conversion efficiency of N719 dye-sensitized solar cell," *Coord. Chem. Rev.* **248**, 1381-1389 (2004) [doi:10.1016/j.ccr.2004.03.006].
[29] S. Hore, C. Vetter, R. Kern, H. Smit, and A. Hinsch, "Influence of scattering layers on efficiency of dye-sensitized solar cells," *Sol. Energy Mater. Sol. Cells* **90**, 1176-1188 (2006) [doi:10.1016/j.solmat.2005.07.002].
[30] C. P. Hsu, K. M. Lee, J. T. W. Huang, C. Y. Lin, C. H. Lee, L. P. Wang, S. Y. Tsai, and K. C. Ho, "EIS analysis on low temperature fabrication of TiO_2 porous films for dye-sensitized solar cells," *Electrochim. Acta* **53**, 7514-7522 (2008) [doi:10.1016/j.electacta.2008.01.104].
[31] L. H. Hu, S. Y. Dai, J. Weng, S. F. Xiao, Y. F. Sui, Y. Huang, S. H. Chen, F. T. Kong, X. Pan, L. Y. Liang, and K. J. Wang, "Microstructure design of nanoporous TiO_2 photoelectrodes for dye-sensitized solar cell modules," *J. Phys. Chem. B* **111**, 358-362 (2007) [doi:10.1021/jp065541a].
[32] S. Ito, M. Nazeeruddin, P. Liska, P. Comte, R. Charvet, P. Péchy, M. Jirousek, A. Kay, S. Zakeeruddin, and M. Grätzel, "Photovoltaic characterization of dye-sensitized solar cells: effect of device masking on conversion efficiency," *Prog. Photovoltaics Res. Appl.* **14**, 589–601 (2006) [doi:10.1002/pip.683].
[33] S. Ito, M. Nazeeruddin, S. Zakeeruddin, P. Péchy, P. Comte, M. Grätzel, T. Mizuno, A. Tanaka, and T. Koyanagi, "Study of dye-sensitized solar cells by scanning eletron

micrograph observation and thickness optimazation of porous TiO_2 electrodes," *Int. J. Photoenergy* **2009**, p. 517609 (2009) [doi:10.1155/2009/517609].

[34] J. T. Jiu, F. M. Wang, M. Sakamoto, J. Takao, and M. Adachi, "Performance of dye-sensitized solar cell based on nanocrystals TiO_2 film prepared with mixed template method," *Sol. Energy Mater. Sol. Cells* **87**, 77-86 (2005) [doi:10.1016/j.solmat.2004.06.011].

[35] H. J. Koo, J. Park, B. Yoo, K. Yoo, K. Kim, and N. G. Park, "Size-dependent scattering efficiency in dye-sensitized solar cell," *Inorg. Chim. Acta* **361**, 677-683 (2008) [doi:10.1016/j.ica.2007.05.017].

[36] W. W. Tan, X. Yin, X. M. Zhou, J. B. Zhang, X. R. Xiao, and Y. Lin, "Electrophoretic deposition of nanocrystalline TiO_2 films on Ti substrates for use in flexible dye-sensitized solar cells," *Electrochim. Acta* **54**, 4467-4472 (2009) [doi:10.1016/j.electacta.2009.03.037].

[37] L. Yang, Y. Lin, J. G. Jia, X. R. Xiao, X. P. Li, and X. W. Zhou, "Light harvesting enhancement for dye-sensitized solar cells by novel anode containing cauliflower-like TiO_2 spheres," *J. Power Sources* **182**, 370-376 (2008) [doi:10.1016/j.jpowsour.2008.03.013].

[38] Z. P. Zhang, S. Ito, B. O'Regan, D. B. Kuang, S. M. Zakeeruddin, P. Liska, R. Charvet, P. Comte, M. K. Nazeeruddin, P. Pechy, R. Humphry-Baker, T. Koyanagi, T. Mizuno, and M. Gratzel, "The electronic role of the TiO_2 light-scattering layer in dye-sensitized solar cells," *Z. Phys. Chem.* **221**, 319-327 (2007) [doi: 10.1524/zpch.2007.221.3.319].

[39] S. Colodrero, A. Mihi, L. Haggman, M. Ocana, G. Boschloo, A. Hagfeldt, and H. Miguez, "Porous one-dimensional photonic crystals improve the power-conversion efficiency of dye-sensitized solar cells," *Adv. Mater.* **21**, 764-770 (2009) [doi:10.1002/adma.200703115].

[40] L. I. Halaoui, N. M. Abrams, and T. E. Mallouk, "Increasing the conversion efficiency of dye-sensitized TiO_2 photoelectrochemical cells by coupling to photonic crystals," *J. Phys. Chem. B* **109**, 6334-6342 (2005) [doi:10.1021/jp044228a].

[41] S. H. A. Lee, N. M. Abrams, P. G. Hoertz, G. D. Barber, L. I. Halaoui, and T. E. Mallouk, "Coupling of titania inverse oals to nanocrystalline titania layers in dye-sensitized solar cells," *J. Phys. Chem. B* **112**, 14415-14421 (2008) [doi:10.1021/jp802692u].

[42] A. Mihi, M. E. Calvo, J. A. Anta, and H. Miguez, "Spectral response of opal-based dye-sensitized solar cells," *J. Phys. Chem. C* **112**, 13-17 (2008) [doi:10.1021/jp7105633].

[43] A. Mihi and H. Miguez, "Origin of light-harvesting enhancement in colloidal-photonic-crystal-based dye-sensitized solar cells," *J. Phys. Chem. B* **109**, 15968-15976 (2005) [doi:10.1021/jp051828g].

[44] S. Nishimura, N. Abrams, B. A. Lewis, L. I. Halaoui, T. E. Mallouk, K. D. Benkstein, J. van de Lagemaat, and A. J. Frank, "Standing wave enhancement of red absorbance and photocurrent in dye-sensitized titanium dioxide photoelectrodes coupled to photonic crystals," *J. Am. Chem. Soc.* **125**, 6306-6310 (2003) [doi:10.1021/ja034650p].

[45] R. Rengarajan, D. Mittleman, C. Rich, and V. Colvin, "Effect of disorder on the optical properties of colloidal crystals," *Phys. Rev. E* **71**, p. 016615 (2005) [doi:10.1103/PhysRevE.71.016615].

[46] C. H. Yip, Y. M. Chiang, and C. C. Wong, "Dielectric band edge enhancement of energy conversion efficiency in photonic crystal dye-sensitized solar cell," *J. Phys. Chem. C* **112**, 8735-8740 (2008) [doi:10.1021/jp801385k].

[47] S. Hore, P. Nitz, C. Vetter, C. Prahl, M. Niggemann, and R. Kern, "Scattering spherical voids in nanocrystalline TiO_2 - enhancement of efficiency in dye-sensitized solar cells," *Chem. Commun.* 2011-2013 (2005) [doi:10.1039/b418658n].

[48] G. Z. Cao, "Popcorn-style solar cells," *Photonics Spectra* **42**, 60-61 (2008).

[49] T. P. Chou, Q. F. Zhang, G. E. Fryxell, and G. Z. Cao, "Hierarchically structured ZnO film for dye-sensitized solar cells with enhanced energy conversion efficiency," *Adv. Mater.* **19**, 2588-2592 (2007) [doi: 10.1002/adma.200602927].

[50] Q. F. Zhang, T. P. Chou, B. Russo, S. A. Jenekhe, and G. Cao, "Polydisperse aggregates of ZnO nanocrystallites: A method for energy-conversion-efficiency enhancement in dye-sensitized solar cells," *Adv. Funct. Mater.* **18**, 1654-1660 (2008) [doi:10.1002/adfm.200701073].

[51] Q. F. Zhang, T. R. Chou, B. Russo, S. A. Jenekhe, and G. Z. Cao, "Aggregation of ZnO nanocrystallites for high conversion efficiency in dye-sensitized solar cells," *Angew. Chem. Int. Ed.* **47**, 2402-2406 (2008) [doi:10.1002/anie.200704919].

[52] Q. F. Zhang, C. S. Dandeneau, S. Candelaria, D. W. Liu, B. B. Garcia, X. Y. Zhou, Y. H. Jeong, and G. Z. Cao, "Effects of Lithium Ions on Dye-Sensitized ZnO Aggregate Solar Cells," *Chem. Mater.* **22,** 2427-2433 (2010) [doi:10.1021/cm9009942].

[53] D. Jezequel, J. Guenot, N. Jouini, and F. Fievet, "Submicrometer zinc-oxide particles - elaboration in polyol medium and morphological-characteristics," *J. Mater. Res.* **10**, 77-83 (1995) [doi:10.1557/JMR.1995.0077].

[54] M. Ryan, "Progress in ruthenium complexes for dye sensitized solar cells," *Platinum Met. Rev.* **53**, 216-218 (2009) [doi:10.1595/147106709X475315].

[55] M. K. Nazeeruddin, A. Kay, I. Rodicio, R. Humphrybaker, E. Muller, P. Liska, N. Vlachopoulos, and M. Gratzel, "Coversion of light to electricity by cis-X2bis(2,2'-bipyridyl-4,4'-dicarboxylate)ruthenium(II) charge-transfer sensitizers (X = CL-, BR-, I-, CN-, and SCN-) on nanocrystalline TiO_2 electrodes," *J. Am. Chem. Soc.* **115**, 6382-6390 (1993) [doi:10.1021/ja00067a063].

[56] A. Guinier, *X-ray Diffraction in Crystals, Imperfect Crystals, and Amorphous Bodies*, Dover Publications, Mineola, New York (1994).

[57] H. C. van de Hulst, *Light Scattering by Small Particles*, Dover Publications, Mineola, New York (1981).

[58] P. Barber and S. Hill, *Light Scattering by Particles: Computational Methods*, World Scientific, Singapore (1990).

[59] P. E. Wolf and G. Maret, "Weak localization and coherent backscattering of photons in disordered media," *Phys. Rev. Lett.* **55**, 2696-2699 (1985) [doi:10.1103/PhysRevLett.55.2696].

[60] H. Cao, J. Y. Xu, D. Z. Zhang, S. H. Chang, S. T. Ho, E. W. Seelig, X. Liu, and R. P. H. Chang, "Spatial confinement of laser light in active random media," *Phys. Rev. Lett.* **84**, 5584-5587 (2000) [doi:10.1103/PhysRevLett.84.5584].

[61] X. H. Wu, A. Yamilov, H. Noh, H. Cao, E. W. Seelig, and R. P. H. Chang, "Random lasing in closely packed resonant scatterers," *J. Opt. Soc. Am. B* **21**, 159-167 (2004) [doi:10.1364/JOSAB.21.000159].

[62] C. Bohren and D. R. Huffman, *Absorption and Scattering of Light by Small Particles*, Wiley, New York (1983).

[63] S. M. Scholz, R. Vacassy, J. Dutta, H. Hofmann, and M. Akinc, "Mie scattering effects from monodispersed ZnS nanospheres," *J. Appl. Phys.* **83**, 7860-7866 (1998) [doi:10.1063/1.367961].

[64] M. Abramowitz and I. Stegun, *Handbook of Mathematical Functions*, Dover Publications, Mineola, New York (1965).

[65] H. Du, "Mie-scattering calculation," *Appl. Opt.* **43**, 1951-1956 (2004) [doi:10.1364/AO.43.001951].

[66] X. W. Sun and H. S. Kwok, "Optical properties of epitaxially grown zinc oxide films on sapphire by pulsed laser deposition," *J. Appl. Phys.* **86**, 408-411 (1999) [doi:10.1063/1.370744].

[67] D. S. Wiersma, P. Bartolini, A. Lagendijk, and R. Righini, "Localization of light in a disordered medium," *Nature* **390**, 671-673 (1997) [doi:10.1038/37757].

[68] M. Gratzel, "Dye-sensitized solar cells," *J. Photochem. Photobiol., C* **4**, 145-153 (2003) [doi:10.1016/S1389-5567(03)00026-1].
[69] X. C. Jiang, T. Herricks, and Y. N. Xia, "Monodispersed spherical colloids of titania: Synthesis, characterization, and crystallization," *Adv. Mater.* **15**, 1205-1209 (2003) [doi:10.1002/adma.200305105].
[70] T. P. Chou, Q. F. Zhang, and G. Z. Cao, "Effects of dye loading conditions on the energy conversion efficiency of ZnO and TiO_2 dye-sensitized solar cells," *J. Phys. Chem. C* **111**, 18804-18811 (2007) [doi:10.1021/jp076724f].
[71] T. P. Chou, Q. F. Zhang, B. Russo, G. E. Fryxell, and G. Z. Cao, "Titania particle size effect on the overall performance of dye-sensitized solar cells," *J. Phys. Chem. C* **111**, 6296-6302 (2007) [doi:10.1021/jp068939f].
[72] P. Raveendran, M. Eswaramoorthy, U. Bindu, M. Chatterjee, Y. Hakuta, H. Kawanami, and F. Mizukami, "Template-free-formation of meso-structured anatase TiO_2 with spherical morphology," *J. Phys. Chem. C* **112**, 20007-20011 (2008) [doi:10.1021/jp805963s].
[73] L. S. Zhong, J. S. Hu, L. J. Wan, and W. G. Song, "Facile synthesis of nanoporous anatase spheres and their environmental applications," *Chem. Commun.* 1184-1186 (2008) [doi:10.1039/b718300c].
[74] S. Brunauer, P. H. Emmett, and E. Teller, "Adsorption of gases in multimolecular layers," *J. Am. Chem. Soc.* **60**, 309-319 (1938) [doi:10.1021/ja01269a023].
[75] N. G. Park, J. van de Lagemaat, and A. J. Frank, "Comparison of dye-sensitized rutile- and anatase-based TiO_2 solar cells," *J. Phys. Chem. B* **104**, 8989-8994 (2000) [doi:10.1021/jp994365l].

Qifeng Zhang received his Ph. D. degree from Peking University, China. He is currently working in University of Washington as an Acting Assistant Professor-Temp. His research interests involve engineering applications of nano-structured materials on electrical devices such as solar cells, UV light-emitting diodes (LEDs), field-effect transistors (FETs), and gas sensors.

Christopher S. Dandeneau earned a bachelor's degree in Applied Physics and Mathematics from Linfield College, and a Master of Materials Science degree from Oregon State University. He is currently is a PhD candidate working on inorganic-organic hybrid solar cells in Materials Science and Engineering Department at University of Washington.

Kwangsuk Park received his B.S. and M.S. degree from Kyungpook National University (South Korea) in 1998 and 2000. After working at Samsung Techwin and LG Electronics Institute of Technology for 7 years, he joined Professor Guozhong Cao group in University of Washington as graduate student in 2008. His current research is synthesis and application of nanomaterials like dye-sensitized solar cells.

Dawei Liu is a Ph.D. candidate in the Department of Materials Science and Engineering, University of Washington, and is supervised by Professor Guozhong Cao. He received his bachelor's degree from the Department of Physics, Nanjing University, China.

Xiaoyuan Zhou obtained her Ph.D. degree from Hong Kong Polytechnic University (China) in 2008. She is currently a Postdoc Research Fellow. Her research interests include the development of novel, highly efficient thermoelectric materials; on the study of solar cell based on nanostructured materials; and on the investigations of provskite-type ferroelectric thin film for tunable microwave devices applications.

Jeong Yoon-Ha is a professor of Electrical Engineering at Pohang University of Science and Technology (POSTECH), South Korea. He is the Vice President of POSTECH and the founder of POSTECH's National Center for Nanomaterials Technology (NCNT).

Guozhong Cao is Boeing-Steiner Professor of Materials Science and Engineering and Adjunct Professor of Chemical and Mechanical Engineering at the University of Washington. He has published over 250 refereed papers, and authored and edited 5 books including "Nanostructures and Nanomaterials". His current research is focused mainly on nanomaterials for energy conversion and storage including solar cells, lithium-ion batteries, supercapacitors, and hydrogen storage materials.